AGU PUBLICATIONS

JGR

Journal of Geophysical Research: Atmospheres

RESEARCH ARTICLE
10.1002/2016JD025286

Key Points:
- The springtime biomass burning activities in Indochina vary with two geographical regions: northern Indochina and southern Indochina
- The interannual variation of biomass burning over northern Indochina is closely related with the changes of PM10 at Mt. Lulin in Taiwan
- The changes of the India-Burma Trough are important to the modulation of the aerosol transport pattern from northern Indochina to Taiwan

Correspondence to:
W.-R. Huang,
wrhuang@ntnu.edu.tw

Citation:
Huang, W.-R., S.-H. Wang, M.-C. Yen, N.-H. Lin, and P. Promchote (2016), Interannual variation of springtime biomass burning in Indochina: Regional differences, associated atmospheric dynamical changes, and downwind impacts, *J. Geophys. Res. Atmos.*, *121*, 10,016–10,028, doi:10.1002/2016JD025286.

Received 27 APR 2016
Accepted 14 AUG 2016
Accepted article online 17 AUG 2016
Published online 5 SEP 2016

Interannual variation of springtime biomass burning in Indochina: Regional differences, associated atmospheric dynamical changes, and downwind impacts

Wan-Ru Huang[1], Sheng-Hsiang Wang[2], Ming-Cheng Yen[2], Neng-Huei Lin[2], and Parichart Promchote[3,4]

[1]Department of Earth Sciences, National Taiwan Normal University, Taipei, Taiwan, [2]Department of Atmospheric Sciences, National Central University, Taoyuan, Taiwan, [3]Department of Agronomy, Kasetsart University, Bangkok, Thailand, [4]Department of Plants, Soils, and Climate, Utah State University, Logan, Utah, USA

Abstract During March and April, widespread burning occurs across farmlands in Indochina in preparation for planting at the monsoon onset. The resultant aerosols impact the air quality downwind. In this study, we investigate the climatic aspect of the interannual variation of springtime biomass burning in Indochina and its correlation with air quality at Mt. Lulin in Taiwan using long-term (2005–2015) satellite and global reanalysis data. Based on empirical orthogonal function (EOF) analysis, we find that the biomass burning activities vary with two geographical regions: northern Indochina (the primary EOF mode) and southern Indochina (the secondary EOF mode). We determine that the variation of biomass burning over northern Indochina is significantly related with the change in aerosol concentrations at Mt. Lulin. This occurs following the change in the so-called India-Burma Trough in the lower and middle troposphere. When the India-Burma Trough is intensified, a stronger northwesterly wind (to the west of the trough) transports the dryer air from higher latitude into northern Indochina, and this promotes local biomass burning activities. The increase in upward motion to the east of the intensified India-Burma Trough lifts the aerosols, which are transported toward Taiwan by the increased low-level westerly jet. Further diagnoses revealed the connection between the India-Burma Trough and the South Asian jet's wave train pattern as well as the previous winter's El Niño–Southern Oscillation phase. This information highlights the role of the India-Burma Trough in modulating northern Indochina biomass burning and possibly predicting aerosol transport to East Asia on the interannual time scale.

1. Introduction

During March and April, widespread agro-residue burning occurs across farmlands in Indochina (red area in Figure 1a) in preparation for planting at the monsoon onset. This burning occurs in conjunction with local hot-dry-stagnant air and generates smoke and haze aerosol pollution, particularly over the valley terrain of the northern peninsula [*Kim Oanh and Leelasakultum*, 2011]. Because the resultant aerosols affect not only the local region but also the air quality downwind, many studies have examined the climate and weather characteristics in association with biomass burning [*Duncan et al*., 2003; *Yen et al*., 2013; *Wang et al*., 2015]. In general, biomass burning occurs over Indochina during the time period from February to April, with a maximum occurrence in March (Figure 1b). After the monsoon rainfall onset in late April, the occurrence of fire events becomes minimal. The annual variation of aerosol concentrations over Indochina depends on the prevailing times of biomass burning [*Gautam et al*., 2013; *Huang et al*., 2013]. Some reports revealed that aerosols generated by biomass burning could be reduced by the increase of precipitation and monsoon circulation due to rainout and washout processes [*Sanap and Pandithurai*, 2015; *Sonkaew and Macatangay*, 2015].

Based on the NOAA's Hybrid Single-Particle Lagrangian-Integrated Trajectory model simulations, earlier studies [*Yu et al*., 2008; *Yen et al*., 2013] demonstrated that the long-range transport of Indochina's biomass burning pollutants has a significant impact on the surface air quality of downstream areas, particularly in Taiwan. The biomass burning emissions are uplifted above the planetary boundary layer through regional convergence at the lower level and strong thermal buoyancy [e.g., *Yen et al*., 2013; *Wang et al*., 2015]. After being lifted, the aerosols are transported to Taiwan by the low-level westerly jet (Figures 1c and 1d) within 2–3 days [e.g., *Cheng et al*., 2013; *Yen et al*., 2013; *Dong and Fu*, 2015]. These aerosol transports can result in significant increase of air pollutant concentrations in Taiwan, as reported by many studies [e.g., *Lee et al*., 2011; *Yen et al*.,

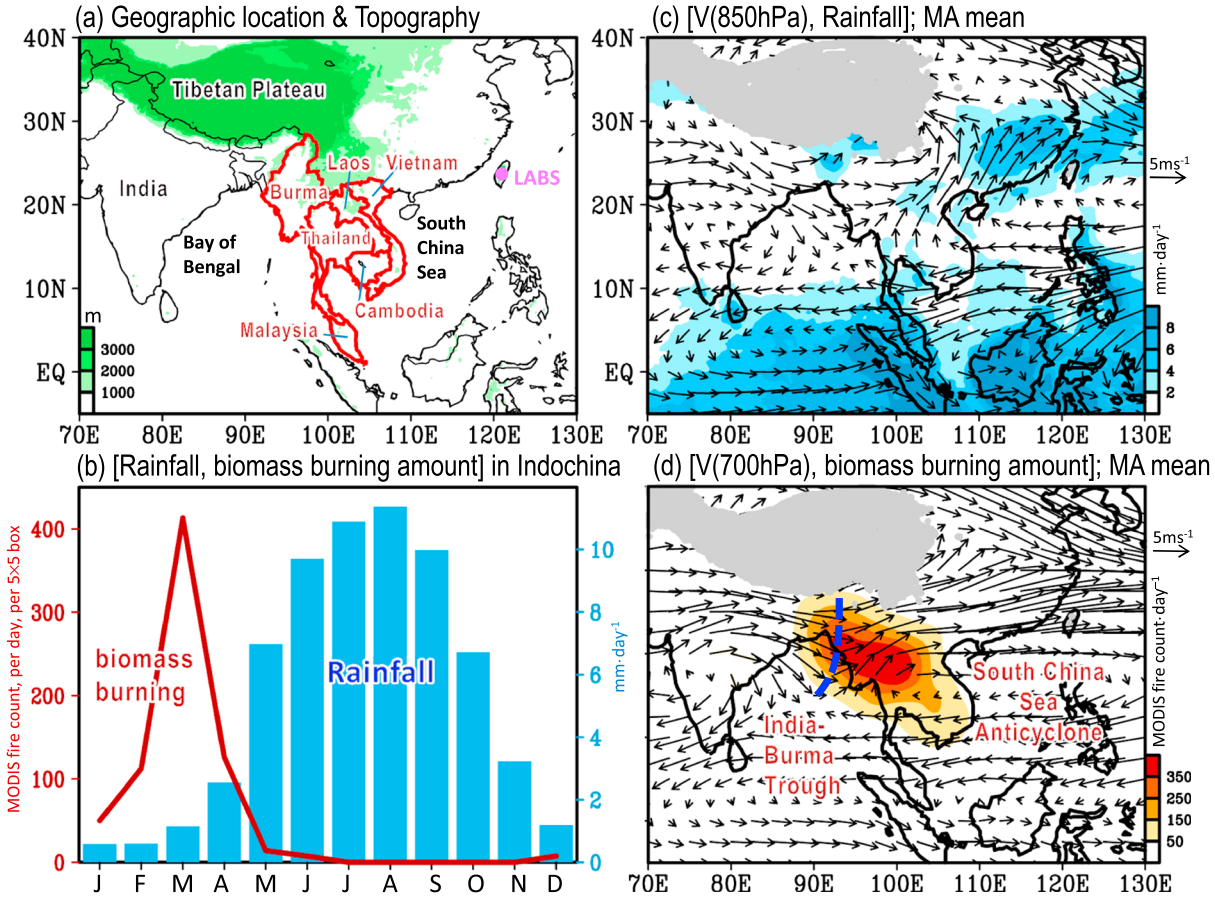

Figure 1. (a) Geographic location of Indochina (red marked area). The location of the Lulin Atmospheric Background Station (LABS; altitude: 2862 m) in Taiwan is marked by the pink dot in Figure 1a. (b) Area-averaged monthly mean rainfall (blue bar) and biomass burning amount (i.e., MODIS fire count; red line) over Indochina. (c) Climatological mean of March and April (hereafter, MA mean) wind vectors at 850 hPa and the MA mean of precipitation (shaded). (d) MA mean of the 700 hPa wind vectors and biomass burning amount (shaded). The blue line in Figure 1d represents the India-Burma Trough.

2013; *Chuang et al.*, 2015]. For example, *Chuang et al.* [2015] noted that the concentrations of particulate matter $(PM)_{2.5}$ and PM_{10} at Mt. Lulin of Taiwan was increased from approximately 15–20 $\mu g\,m^{-3}$ to 53–64 $\mu g\,m^{-3}$ on 12 March 2010 after the arrival of the biomass burning plume from Indochina.

Even though the aforementioned relationship between biomass burning in Indochina and its downwind influences on concentration of air pollutants (e.g., PM_{10} and $PM_{2.5}$) in Taiwan has been reported [e.g., *Yen et al.*, 2013; *Chuang et al.*, 2015], the contribution of the low-level trough over the Bay of Bengal (so-called India-Burma Trough; Figure 1d) on the aerosol transport pattern has not been emphasized. Several studies have suggested that the India-Burma Trough is a key system affecting the weather and climate over Southeast Asia, especially in winter [e.g., *Suo et al.*, 2008; *Suo and Ding*, 2009; *Zhou et al.*, 2009; *Zong et al.*, 2012; *Wang et al.*, 2011; *Li and Zhou*, 2016]. *Suo and Ding* [2009] noted that the India-Burma Trough is generally established in October, is maintained from November to the following February, and peaks from March to May. *Li and Zhou* [2016] further suggested that the interannual variation of winter precipitation over southwest China is modulated by the change of the India-Burma Trough. As inferred from this documented literature, it is likely that the changes in the India-Burma Trough might play an important role in modulating the interannual variation of biomass burning in Indochina and its downwind impacts on the air quality in Taiwan.

In 2007, the Seven SouthEast Asian Studies (7-SEAS) project (http://7-seas.gsfc.nasa.gov/) was established to perform research in the field of aerosol-meteorology and climate interactions from Java through the Malay Peninsula and Southeast Asia to Taiwan [*Reid et al.*, 2013; *Lin et al.*, 2013]. The Lulin Atmospheric Background Station (LABS), located at Mt. Lulin (altitude: 2862 m; 23°28′07″N, 120°52′25″N; http://lulin.tw) in central Taiwan, started operations on April 2006 to provide continuous observations of a variety of aerosol

chemistry parameters, trace gases, etc. The long-term observational data collected by the 7-SEAS project and LABS in Taiwan now provide a great opportunity for studying the relationship between the variations of biomass burning in Indochina and the variations of air quality in Taiwan on an internal interannual time scale.

This study aims to examine the interannual variation of biomass burning in Indochina and its associated atmospheric dynamical changes, with a focus on understanding the role of the India-Burma Trough in modulating the aerosol transport from Indochina to LABS in Taiwan. Considering a large domain from the tropics to 25°N of Indochina (Figure 1a), the atmospheric circulation features important for the modulation of the interannual variation of biomass burning in different subregions of Indochina might be different. This inference, together with the regional differences in the interannual variation of biomass burning and its downwind impacts, will be clarified in the subsequent analysis.

The remainder of this paper is organized as follows. In section 2, the data used for the analyses are described. Section 3 reports the spatial-temporal characteristics of the interannual variation of biomass burning in Indochina, their relations to air quality in Taiwan, and the associated atmospheric circulation features. Discussion is provided in section 4. A summary is given in section 5.

2. Data and Methodology

In this study, the biomass burning activity from 2005 to 2015 is identified by fire data from Moderate Resolution Imaging Spectroradiometer (MODIS; http://modis.gsfc.nasa.gov/) on board NASA's Terra and Aqua satellites. The MOD14 (*Terra*) and MYD14 (*Aqua*) active fire product detects fires in 1 km pixels that are burning at the time of overpass under relatively cloud-free conditions [*Giglio et al*., 2003]. The overpass time for Terra and Aqua are approximately 10:30 and 13:30 local time, respectively. The daily fire counts are calculated from the sum of the MOD14 and MYD14 data sets. Because the MODIS fire count data exhibit some quality problem in the early 2000s [*Giglio*, 2013; *Giglio et al*., 2013], only data from 2005 onward were used. For a detailed review of the MODIS fire count data, please refer to *Giglio* [2013].

To further validate the representativeness of MODIS fire count for biomass burning activities over Indochina, we also examined the biomass burning dry matter emissions (hereafter, biomass burning emissions) provided by the Global Fire Emissions Database, version 4 (GFED4s; http://globalfiredata.org/data.html) [*Giglio et al*., 2013]. The GFED4s provides various types of biomass burning emissions, and this study only used the changes of total amount of biomass burning emissions (i.e., the summation of all types). It should be noted that MODIS exhibits a limit in capturing peat burning [*Giglio et al*., 2010]; however, we considered this limitation neglectable because the proportion of peat burning to total biomass burning emissions over Indochina is small [e.g., *Shi and Yamaguchi*, 2014]. As will be shown in Figure 3 (discussed later), the interannual variation of the GFED4s' total biomass burning emissions matches well with that of the MODIS fire count over Indochina. This result indicates that MODIS fire count can represent biomass burning activities over Indochina, consistent with *Yu et al.* [2008] and *Wang et al.* [2015].

To examine the impact of biomass burning on downwind air quality, we selected LABS as the representative location because the transportation of the biomass burning plume from Indochina to Taiwan has been well documented by the measurement data collected from this station [e.g., *Ou Yang et al*., 2014, and references therein]. The instrument for the PM_{10} and $PM_{2.5}$ mass concentration is the tapered element oscillating microbalance (RP 1400a, USA). In this study, we used only PM_{10} data (~10 years) because of its longer record compared to $PM_{2.5}$ data (~3 years).

For the observational precipitation, we used 3 hourly Tropical Rainfall Measuring Mission (TRMM) 3B42 satellite precipitation [*Huffman et al*., 2007]. TRMM 3B42 data have been widely used for the depiction of rainfall variation over South and East Asia [*Hong et al*., 2005; *Zhou et al*., 2008; *Huang and Chan*, 2012; *Huang and Wang*, 2014]. For the meteorological data (including wind fields and humidity), we used the National Centers for Environmental Prediction–Department of Energy (NCEP-DOE) Reanalysis 2 [*Kanamitsu et al*., 2002]. The calculation of the moisture flux from NCEP-DOE Reanalysis 2 is based on equation (1):

$$Q = \frac{1}{g}\left(\int_{300}^{p_s} Vq\ dp\right), \tag{1}$$

where V denotes the horizontal wind vectors, q is the specific humidity, g is the gravity, and p is the pressure level [*Chen et al*., 1988]. Following *Chen et al.* [1988], the moisture flux can be separated into rotational (Q_R)

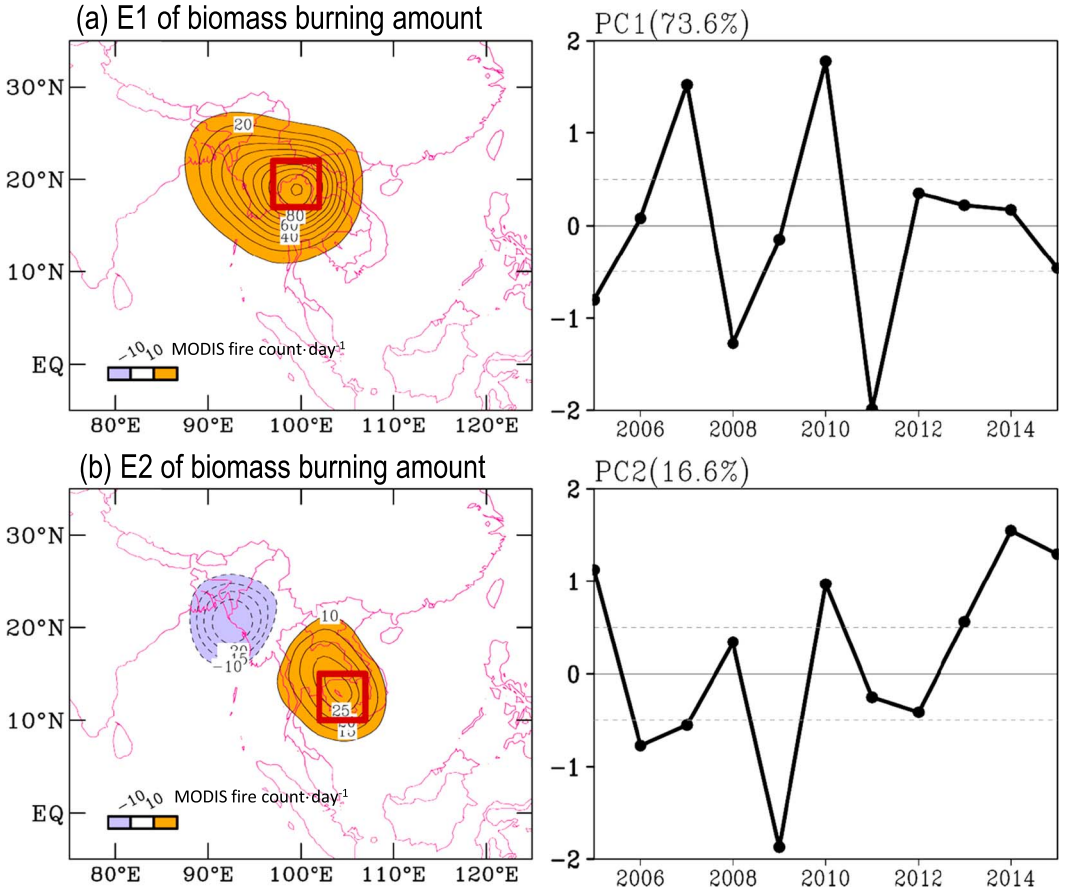

Figure 2. (a) The first-principle mode of the empirical orthogonal function (EOF) analysis on the anomalies of springtime (i.e., MA mean) biomass burning activities during 2005~2015. The eigenvector and eigencoefficient are given in the left and right plots, respectively. (b) Similar to Figure 2a but for the second-principle mode. In E1 (E2), the domain of the maximum variation center in northern (southern) Indochina covering 17–22°N, 97–102°E (10–15°N, 102–107°E) is marked.

and divergent (Q_D) components, which can be further expressed in terms of the stream function (ψ_Q) and potential function (χ_Q) of the moisture flux:

$$Q = Q_R + Q_D = \hat{k} \times \nabla\psi_Q + \nabla\chi_Q, \tag{2}$$

$$\nabla^2\psi_Q = \hat{k} \cdot \nabla \times Q, \tag{3}$$

$$\nabla^2\chi_Q = \nabla \cdot Q. \tag{4}$$

The fields of ψ_Q and χ_Q are obtained by solving the Poisson equation for equations (3) and (4).

Hereafter, unless noted otherwise, the variables used for examination are the monthly means of March and April (MA mean) during the time period of 2005–2015. The anomaly of a variable designates the removal of climatological monthly mean from each month. The index of northern Indochina biomass burning activities was defined as the amount of MODIS fire count over the domain of 17–22°N, 97–102°E (red box in Figure 2a), while the index of southern Indochina biomass burning activities was defined as the amount of MODIS fire count over the domain of 10–15°N, 102–107°E (red box in Figure 2b). The selection of these two specific domains was based on the analysis in Figure 2, as explained later.

3. Results

3.1. Characteristics of Biomass Burning in Indochina and Its Downwind Impact

Figure 1d shows the climatological mean distribution of biomass burning activities (i.e., the MODIS fire count) in Indochina averaged over the focused time period. Visually, the amount of biomass burning activities is

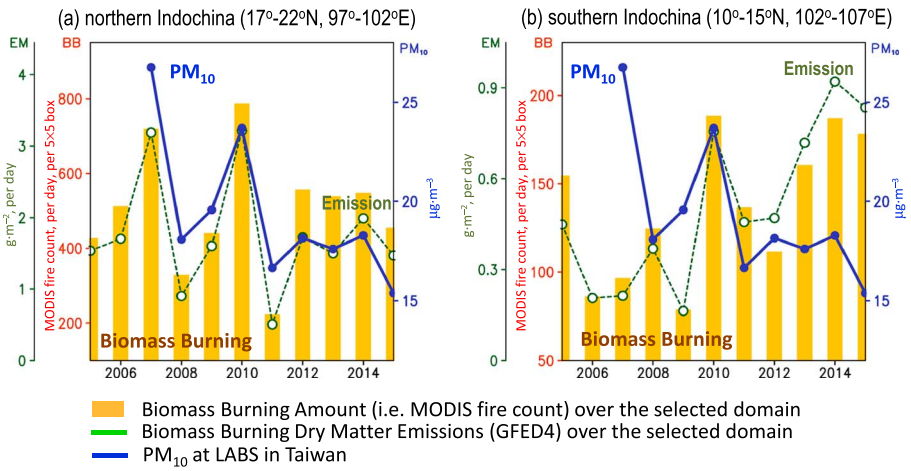

Figure 3. Time series of MA mean of biomass burning activities (bar) and total biomass burning dry matter emissions (green dashed line) over the two selected domains: (a) northern Indochina (17–22°N, 97–102°E; marked in Figure 2a) and (b) southern Indochina (10–15°N, 102–107°E; marked in Figure 2b). In Figures 3a and 3b, the blue line represents the time series of MA mean of PM_{10} at LABS in Taiwan.

larger over northern Indochina, covering most of Burma and northern Thailand, than over southern Indochina. To clarify how these biomass burning activities varied on the interannual time scale, we applied empirical orthogonal function (EOF) analysis on the anomalies of biomass burning activities for the time period of 2005–2015 (Figure 2). The EOF analysis was based on singular-value decomposition (SVD) approach. The SVD approach, which avoids having to compute the covariance matrix directly, provides an optimal way for data sets with a large spatial dimension [*Hannachi et al*., 2007]. Any missing space/time data were removed before applying the SVD approach. For the detailed review of the EOF analysis (including historical background, formulation and computation, and application), please refer to *Hannachi et al.* [2007].

In Figure 2, only the results of the first two EOF modes, together explaining approximately 90% of the total interannual variability of biomass burning activities, are presented. Spatially, the first EOF mode shows that the variation is mainly over northern Indochina, with a largest variation center over northern Thailand (Figure 2a). Corresponding to this spatial distribution, the temporal variation of Figure 2a shows that more (less) biomass burning likely occurred over northern Indochina in the years of 2007 and 2010 (2005, 2008, 2011, and 2015). In contrast, it can be inferred from the spatial-temporal patterns of the second EOF mode (Figure 2b) that over southern Indochina more (less) biomass burning occurred in the years of 2005, 2010, and 2013–2015 (2006, 2007, 2009, and 2012). Additionally, Figure 3 shows the time series of biomass burning activities over the major variation domain of northern Indochina (17–22°N, 97–102°E; marked in Figure 2a) and southern Indochina (10–15°N, 102–107°E; marked in Figure 2b). Consistent with that implied from Figure 2, the results of Figure 3 confirm that the interannual variation of biomass burning activities over northern Indochina is different to that over southern Indochina.

To understand which subregion of biomass burning has a larger impact on the aerosol concentration in Taiwan, we further compared the time series of PM_{10} at LABS in Taiwan (blue lines) with the time series of biomass burning activities (bars)/emissions (green dashed lines) over the major variation domain of northern Indochina (Figure 3a) and southern Indochina (Figure 3b). Notably, the fluctuation of PM_{10} at LABS in Taiwan seems to match better with the fluctuation of biomass burning activities/emissions over northern Indochina than over southern Indochina. More specifically, the maximum (minimum) of PM_{10} at LABS in Taiwan occurred in the years of 2007 and 2010 (2008, 2011, and 2015), when the maximum (minimum) of biomass burning activities/emissions occurred over northern Indochina. Statistically, the temporal correlation coefficient between the interannual variation (i.e., linear trend removed) of PM_{10} at LABS in Taiwan and the biomass burning activities/emissions over northern Indochina is approximately 0.86/0.81 (significant at the 95% confidence interval). Such a temporal variation of PM_{10} is found to be less related to the temporal variation of biomass burning activities/emissions over southern Indochina (the correlation between the two time series in Figure 3b is only −0.15/−0.14). These findings (Figures 2 and 3) highlight the importance of

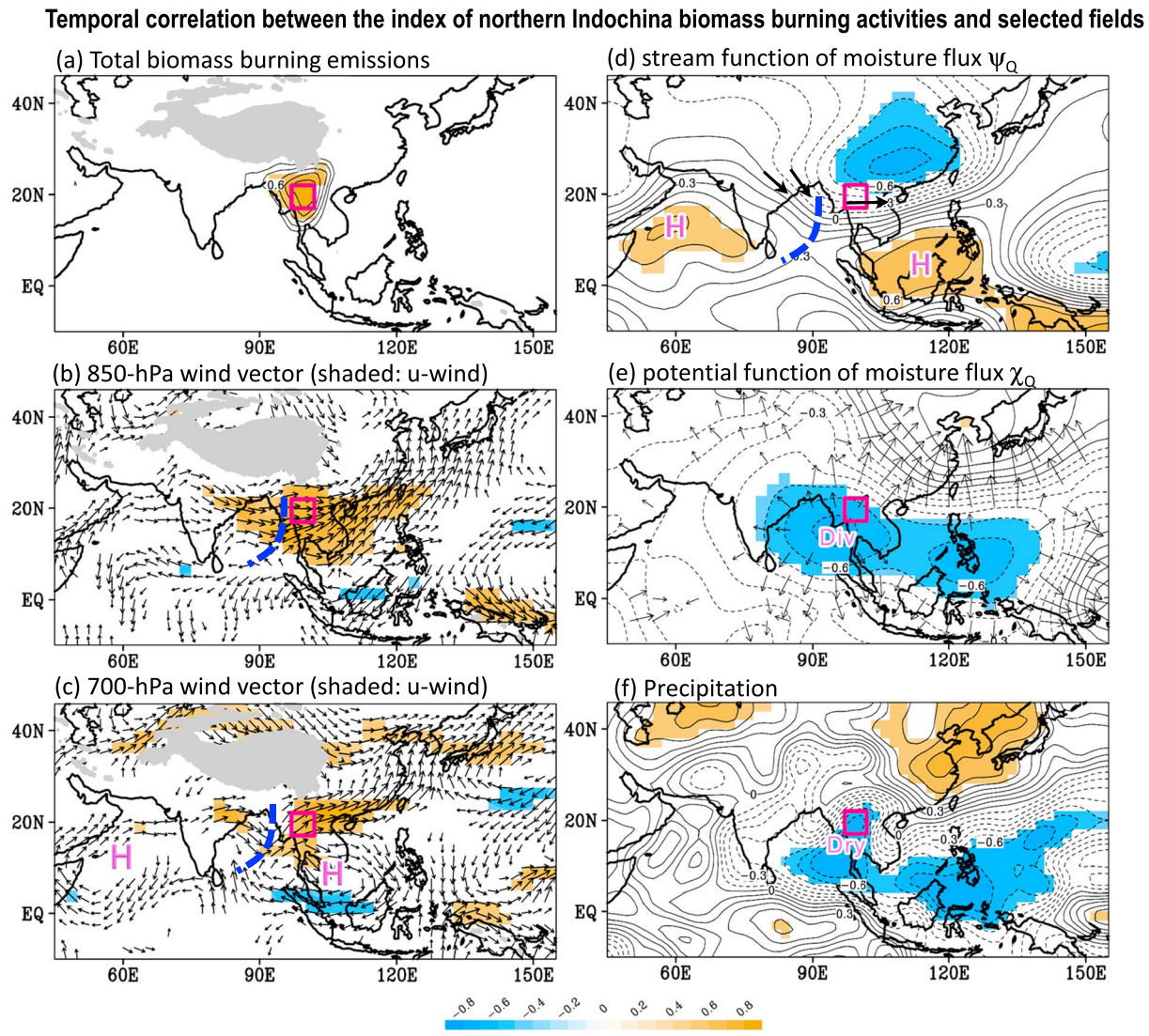

Figure 4. Temporal correlation coefficient between the MA mean index of northern Indochina biomass burning activities (i.e., the amount of MODIS fire count over the domain of 17–22°N, 97–102°E; red boxed area) and six selected variables: (a) GFDE4s total biomass burning dry matter emissions, (b) 850 hPa wind circulation *V* (850 hPa), (c) 700 hPa wind circulation *V* (700 hPa), (d) stream function of the moisture flux ψ_Q, (e) potential function of the moisture flux χ_Q, and (f) precipitation *P* extracted from TRMM observations. The time period of correlation is from 2005 to 2015. Only the areas with significant changes (at the 90% confidence interval) are shaded/shown. The color scale of Figures 4a–4f is given in the bottom plot.

considering regional differences in the discussions of the remote impact of Indochina's biomass burning on the air quality in Taiwan.

3.2. The Associated Atmospheric Circulation Features

Next, we examined the atmospheric circulation changes that are associated with the change of biomass burning over northern Indochina. Here the index of northern Indochina biomass burning activities (i.e., the amount of MODIS fire count over the domain of 17–22°N, 97–102°E) is correlated with the following associated fields: total biomass burning emissions (Figure 4a), 850 hPa wind circulation (Figure 4b), 700 hPa wind circulation (Figure 4c), stream function of the moisture flux ψ_Q (Figure 4d), potential function of the moisture flux χ_Q (Figure 4e), and precipitation (Figure 4f). It is noted that the increase in biomass burning activities/emissions over northern Indochina (Figure 4a) is associated with the intensification of the India-Burma Trough in the lower and middle troposphere (Figures 4b and 4c). In conjunction with such circulation change, both the northwesterly wind behind (to the west) the India-Burma Trough and the westerly/southwesterly wind ahead (to the east) of the India-Burma Trough are intensified relative to the

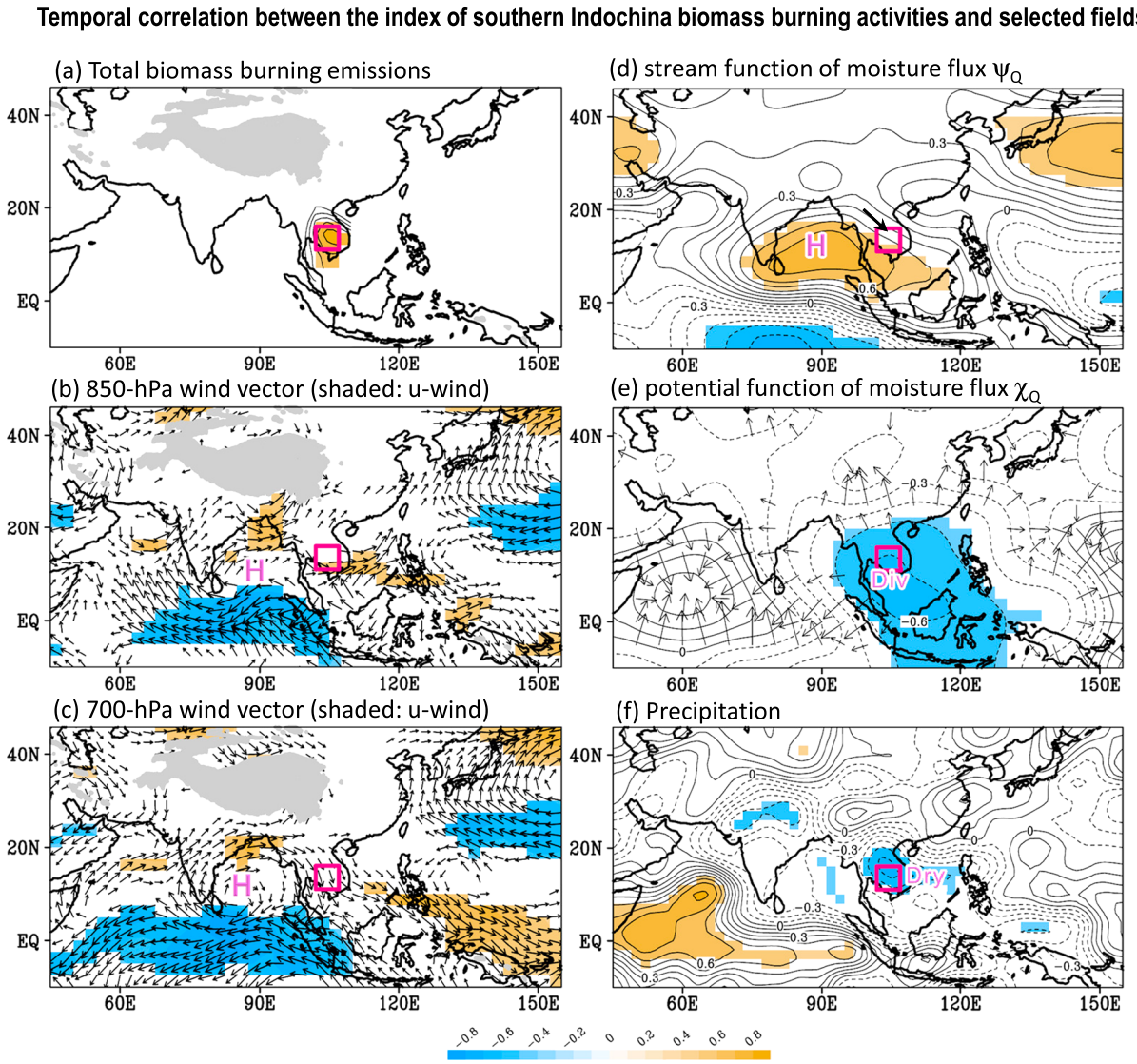

Figure 5. Similar to Figure 4 but for the temporal correlation coefficient between the MA mean index of southern Indochina biomass burning activities (i.e., the amount of MODIS fire count over the domain of 10–15°N, 102–107°E; boxed area) and six selected variables: (a) GFDE4s total biomass burning dry matter emissions, (b) *V* (850 hPa), (c) *V* (700 hPa), (d) ψ_Q, (e) χ_Q, and (f) precipitation *P* extracted from TRMM observations. The time period of correlation is from 2005 to 2015. Only the areas with significant changes (at the 90% confidence interval) are shaded/shown. The color scale of Figures 5a–5f is given in the bottom plot.

climatological mean in the lower and middle troposphere (Figures 4b and 4c). A further examination on the associated change of ψ_Q (Figure 4d) has indicated that the increase in northwesterly wind behind the India-Burma Trough could advect dryer air from the higher latitude to northern Indochina. This would facilitate a moisture divergence center to be formed over the west coast of Indochina, as revealed by the associated change of χ_Q (Figure 4e). Furthermore, such a suppression of the moisture supply from the Bay of Bengal would result in less precipitation to be formed over northern Indochina (Figure 4f), and this dryer condition can help promote the local biomass burning activities (Figure 4a). The argument that less precipitation favors more biomass burning is also suggested by *Dong and Fu* [2015] but for the change of biomass burning accumulated over "entire" Indochina.

Figure 5 presents the correlation maps between the index of southern Indochina biomass burning activities (i.e., the amount of MODIS fire count over the domain of 10–15°N, 102–107°E) and the six selected fields used for northern Indochina (Figure 4). It is noted that the increase in biomass burning activities/emissions over southern Indochina (Figure 5a) is associated with the appearance of an anticyclone system over the Bay of

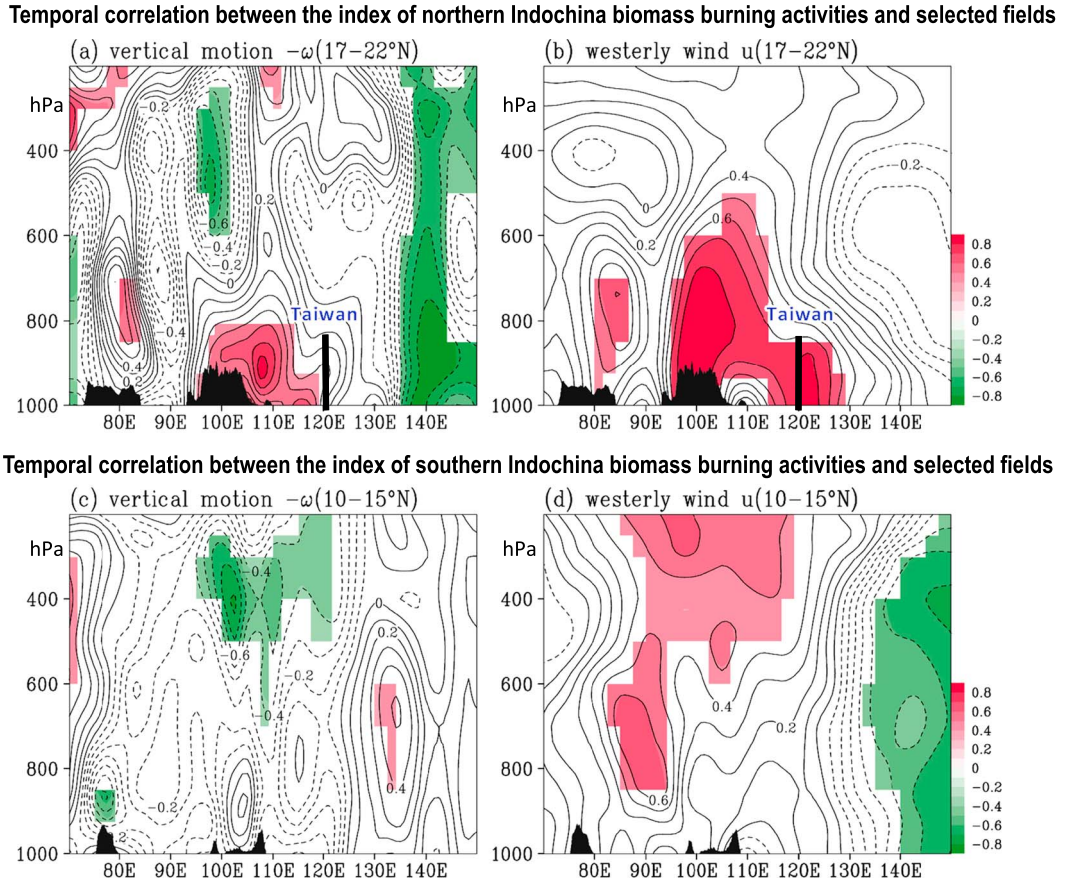

Figure 6. Temporal correlation coefficient between the MA mean index of northern Indochina biomass burning activities (defined in Figure 4) and two selected variables: (a) multilevel vertical motion ($-\omega$; the positive values denote the upward motions) and (b) multilevel westerly wind (u) averaged over 17–22°N. (c and d) Similar to Figures 6a and 6b, respectively, but for the temporal correlation coefficient between the MA mean index of southern Indochina biomass burning activities (defined in Figure 5) and the selected $-\omega$ and u averaged over 10–15°N. The time period of correlation is from 2005 to 2015. The topography is marked. Only the areas with significant changes (at the 90% confidence interval) are shaded.

Bengal in the lower and middle troposphere (Figures 5b and 5c). In conjunction with the Bay of Bengal anticyclone system, the northerly wind is intensified over southern Indochina. Such a circulation change could advect the dryer air from higher latitude to southern Indochina, as noted from the associated change of ψ_Q (Figure 5d). As a result, the moisture flux is divergent over south of the South China Sea (Figure 5e), and less precipitation has occurred over southern Indochina (Figure 5f). Obviously, these circulation changes that are important for the modulation of biomass burning over southern Indochina (Figure 5) are very different to those important for the modulation of biomass burning over northern Indochina (Figure 4). This finding explains why the interannual variation of biomass burning over Indochina is locally dependent.

It should be mentioned that to be transported to Taiwan, the air pollution created by Indochina's biomass burning has to be uplifted to the level with a stronger westerly jet [e.g., *Yen et al*., 2013; *Dong and Fu*, 2015]. Thus, to clarify why the biomass burning over northern Indochina (as compared to that over southern Indochina) has a larger impact on the PM_{10} in Taiwan, we further examined the relationship between the change in vertical motion ($-\omega$; positive value denotes upward motion) and the change in index of northern Indochina biomass burning activities (defined in section 2) The result (Figure 6a) shows that the change in northern Indochina's biomass burning activities is positively correlated to the change in upward motion over the area between Indochina and Taiwan at levels up to 700 hPa. This finding, together with Figures 4e and 4f, implies that more active but dryer upward motion occurred over northern Indochina in the years with greater biomass burning. After the air pollution is uplifted to upper levels, the increase in the westerly wind ahead of the intensified India-Burma Trough (e.g., Figures 4b and 4c), which appeared in the levels up to 500 hPa

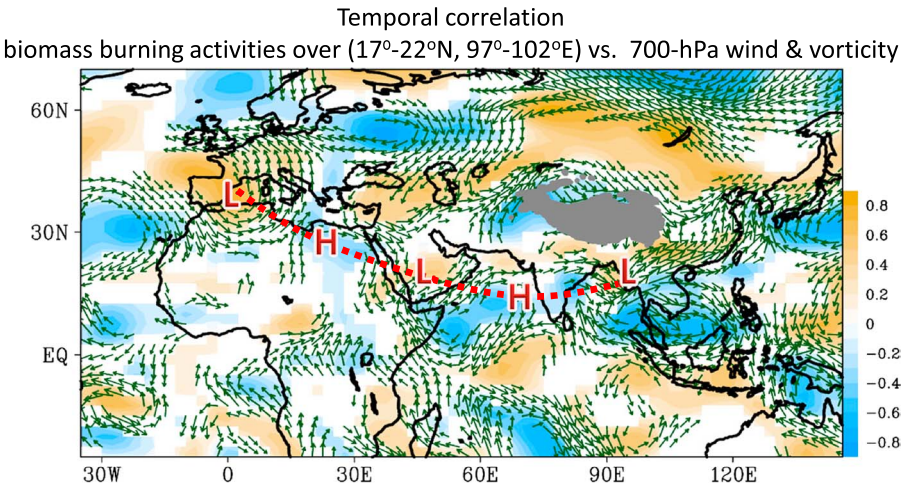

Figure 7. Correlation maps of the 700 hPa wind (vectors) and vorticity (shading) fields with the MA mean index of northern Indochina biomass burning activities (defined in Figure 4). The time period used for correlation is from 2005 to 2015. Only the areas with significant changes (at the 90% confidence interval) are shown.

(Figure 6b), can then help transport the PM_{10} from northern Indochina to Taiwan. In comparing Figures 6a and 6b, there is no clear positive relationship between the change in southern Indochina's biomass burning activities and the change in local upward motion (Figure 6c) or the change in the westerly jet over the area between Indochina and Taiwan (Figure 6d). As a result of the differences between Figures 6a and 6b and Figures 6c and 6d, the change in southern Indochina's biomass burning is not as important as the change in northern Indochina's biomass burning in terms of the change of PM_{10} at LABS in Taiwan.

Notably, in addition to the interannual variation, the PM_{10} at LABS in Taiwan seems to be modulated by a decreasing trend (see Figure 3). However, the time period of 2007–2015 is too short to reasonably identify the existence of such a trend. A further examination on this issue is suggested in the future when a longer period of data is available.

4. Discussion

From section 3, it can be concluded that the change of the India-Burma Trough plays an important role in modulating the interannual variation of biomass burning activities over northern Indochina and its impact on PM_{10} at LABS in Taiwan. Thus, it is important to understand what might cause the change in the India-Burma Trough on the interannual time scale. The recent study of *Li and Zhou* [2016] suggested that the interannual variation of the wintertime (December to the following February) India-Burma Trough is part of the South Asian jet wave train and is modulated by El Niño–Southern Oscillation (ENSO) via the Philippine Sea anticyclone. Here we will clarify if the change of the springtime (March and April) India-Burma Trough is also connected to the change of the South Asian jet wave train and ENSO.

Figure 7 shows the correlation map of the 700 hPa vorticity [i.e., ζ (700 hPa)] and the wind vectors associated with the index of northern Indochina's biomass burning activities (defined in section 2). It is interesting to note that ζ (700 hPa) over the area of the India-Burma Trough is positively correlated with ζ (700 hPa) over the western Mediterranean Sea and Saudi Arabia and negatively correlated with ζ (700 hPa) over the eastern Mediterranean Sea and the Arabian Sea. A better illustration of such a wave train can be revealed in the correlation map of the 700 hPa stream function [i.e., ψ (700 hPa)] with the northern Indochina's biomass burning index, as shown in Figure 8a. By comparing this springtime wave train pattern (Figure 8a) with the wintertime wave train pattern identified in *Li and Zhou* [2016], it is noted that the former also appeared along the South Asian jet but with different variation centers. Such a difference might be attributed to the seasonal variation of the South Asian jet.

Previous studies suggested that the propagation of the Rossby wave from the Mediterranean Sea to the Bay of Bengal is one of the key mechanisms for the enhancement of the India-Burma Trough in wintertime [*Suo*

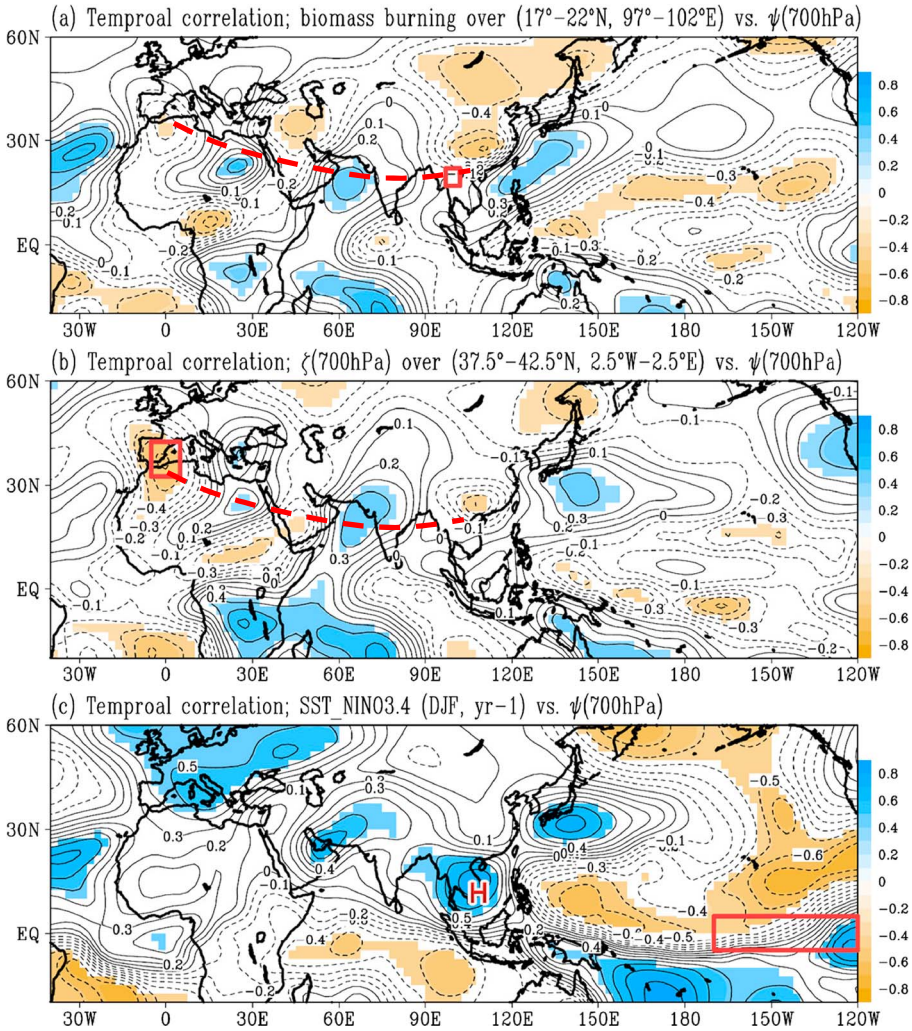

Figure 8. Correlation maps of the MA (March and April) mean stream function ψ at 700 hPa with (a) the MA mean biomass burning activities averaged over 17–22°N, 97–102°E; (b) the MA mean 700 hPa vorticity averaged over 37.5°W–42.5°E, 2.5°W–2.5°E; and (c) the previous winter (DJF, year–1) sea surface temperature averaged over the Niño3.4 region. The time period used for correlation is from 2005 to 2015. Only the areas with significant changes (at the 90% confidence interval) are shaded.

et al., 2008; *Li and Zhou*, 2016]. To clarify if this is also true for the enhancement of the India-Burma Trough in the springtime, we used the area-averaged ζ (700 hPa) over the western Mediterranean Sea (37.5°N–42.5°N, 2.5°W–2.5°E) as an index to correlate with ψ (700 hPa) for March and April of 2005–2015. As revealed in Figure 8b, the wave train pattern with an upstream source over the western Mediterranean Sea propagates downstream across the Mediterranean Sea, Saudi Arabia, and Arabian Sea to the area covering the northern Bay of Bengal, northern Indochina, and south China. This pattern is consistent with that shown in Figure 8a, suggesting that the propagation of such a wave from the western Mediterranean Sea can modulate the change of the India-Burma Trough in the springtime.

We also examined the possible modulation from the downstream ENSO signal to the India-Burma Trough by using the wintertime sea surface temperature (SST) averaged over the Niño3.4 region as an index to correlate the following springtime ψ (700 hPa); the result is given in Figure 8c. It is found that the change of wintertime SST over the Niño3.4 region is positively related to the change of the following springtime anticyclone over the area covering most of the South China Sea (hereafter, South China Sea anticyclone (SCSA)). Consistent with this finding, the bubble chart given in Figure 9 shows that during an El Niño (La Niña) event, a stronger (weaker) SCSA in the following springtime can be expected [e.g., *Wang and Zhang*, 2002]. As noted from

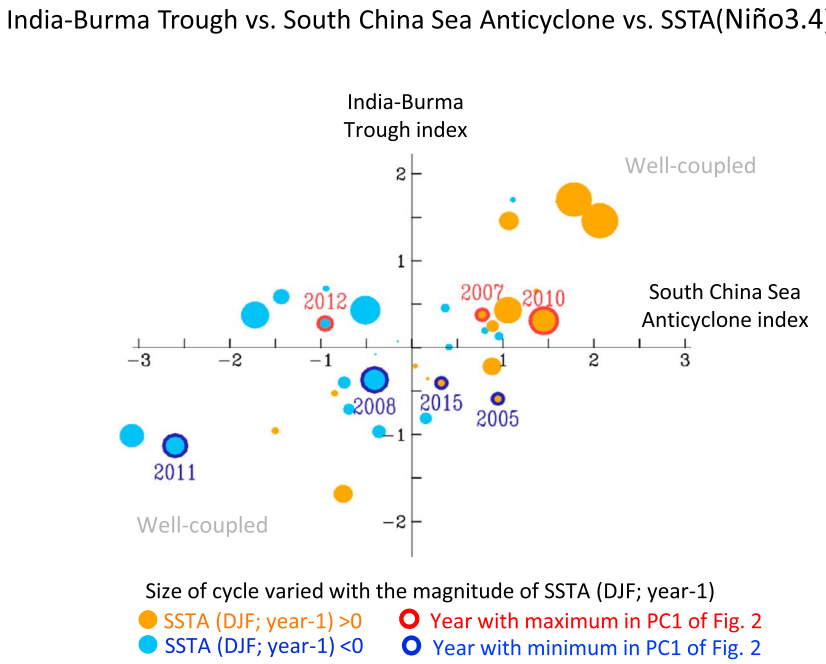

Figure 9. Bubble plot of the springtime (March and April mean) India-Burma Trough index (defined as the area-averaged 700 hPa vorticity, ζ, over 20–30°N, 85–110°E) and the corresponding South China Sea anticyclone index (defined as the "negative" 700 hPa vorticity, $-\zeta$, area averaged over 5–15°N, 95–120°E) during 1979–2015. The explanation for examining the changes over the longer time period (1979–2015) is given in the manuscript. The orange (blue) bubbles are the positive (negative) sea surface temperature anomalies (SSTAs) over the Niño3.4 region in the previous winter, with the size of the bubbles indicating the magnitude of the SSTA. The red (blue) open circles are the years with maximum (minimum) PC1 values of Figure 2.

Figures 1d and 7, the existence of SCSA can help strengthen the westerly jet ahead of the India-Burma Trough [e.g., *Wang et al*., 2011]. In other words, the change in the springtime India-Burma Trough can be modulated by the previous winter's ENSO signal from the tropical East Pacific via the SCSA. To better illustrate the relationship between the SCSA and ENSO, a longer time period (1979–2015) of NCEP-DOE Reanalysis 2 data is used for constructing Figure 9. Details of how the SCSA is established during El Niño development can be found in *Wang and Zhang* [2002].

Finally, we compared the changes of the India-Burma Trough, SCSA, and biomass burning activities over northern Indochina by the bubble chart given in Figure 9. It is noted that in the years with strengthening in both the India-Burma Trough and SCSA (i.e., 2007 and 2010), the amount of biomass burning over northern Indochina is greater than other years with an increase in the India-Burma Trough (i.e., 2012). Consistent with this finding, in the years with weakening in both the India-Burma Trough and SCSA (i.e., 2008 and 2011), the amount of biomass burning over northern Indochina is lower than in other years with a decrease in the India-Burma Trough (i.e., 2005 and 2015). Based on these results, it is suggested that even though the changes of the India-Burma Trough do not always follow the SCSA changes (or the ENSO signal changes), monitoring the SCSA changes (or the ENSO signal changes) does aid in the prediction of the interannual variation of biomass burning over northern Indochina and its impact on PM_{10} in Taiwan. For instance, weakened SCSA and abnormally low biomass burning in 2011 (Figures 2a and 3a) are found consistently with the unusually high 2011 premonsoon rainfall, particularly in March, over northern Thailand [*Promchote et al*., 2015]. This likely suggests that high precipitation can reduce the burning activities over northern Indochina.

It should be noted that although our study reveals the correlations among biomass burning, the India-Burma Trough, and SCSA, there are some additional factors, such as land use change [*Reid et al*., 2013], that might be involved in the changes of biomass burning. For instance, maize-cultivated lands were largely expanded in 2007 over the mountainous terrain in northern Thailand, Myanmar, and Lao, promoted by the high grain price [*Food and Agriculture Organization of the United Nations*, 2016] and private companies; crop residue burning was probably largely increased in this year.

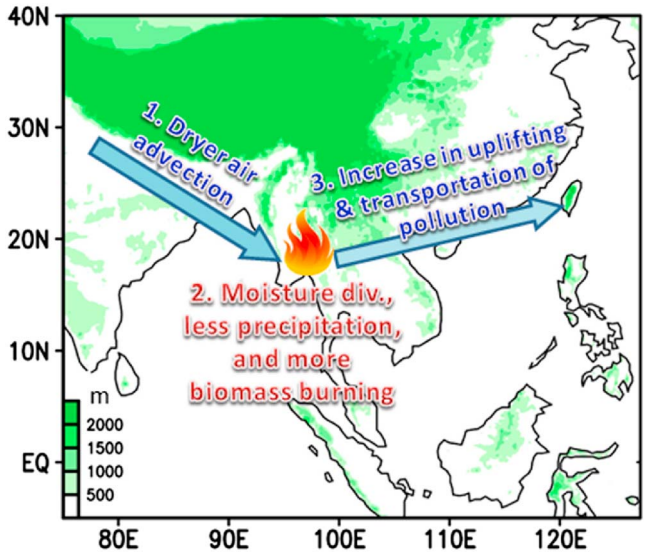

Figure 10. Schematic diagram for illustrating how an intensified India-Burma Trough modulates the occurrence of biomass burning in northern Indochina and its downwind impact on Taiwan. The numbers of 1~3 represent the order of the process. Step 1: an increase in northwesterly wind, behind (to the west) the intensified India-Burma Trough, advects the dryer air from higher latitude to northern Indochina. Step 2: the dryer condition (i.e., less precipitation and moisture divergence) promotes local biomass burning activities. Step 3: the increase in upward motion, ahead (to the east) of the intensified India-Burma Trough, helps uplift the polluted air to the free troposphere, in which the associated increase in the westerly jet transports the PM_{10} from northern Indochina to Taiwan.

5. Summary

In this study, the spatial-temporal characteristics of the interannual variation of biomass burning in Indochina and its downwind impact on PM_{10} at LABS (a high-mountain station) in Taiwan are examined. Diagnoses show that biomass burning activities in Indochina vary with two geographical regions: a primary region in northern Indochina and a secondary region in southern Indochina. PM_{10} at LABS in Taiwan is mainly associated with the interannual variation of biomass burning over northern Indochina but not over southern Indochina.

Changes in biomass burning over northern Indochina and southern Indochina are found to be modulated by different types of atmospheric circulation changes. It is noted that the role of the India-Burma Trough is important to the changes of northern Indochina's biomass burning activities and its associated aerosol transport pattern. As summarized in Figure 10, our results show that in the years with an intensified India-Burma Trough, an increase in northwesterly wind over the southwest side of the Tibetan Plateau (i.e., behind the India-Burma Trough) can advect dryer air from higher latitude to northern Indochina. The associated dryer condition promotes local biomass burning activities. Furthermore, ahead of the intensified India-Burma Trough, the associated increase in upward motion helps uplift the polluted air to the free troposphere, in which the associated increase in the westerly jet transports the PM_{10} from northern Indochina to Taiwan. As for the change in the springtime India-Burma Trough, we noted that it is not only teleconnected with the upstream wave trains from the western Mediterranean Sea but also modulated by the previous winter's ENSO signal from the tropical East Pacific via the South China Sea anticyclone.

The findings of this study are an important step forward in understanding the role of the India-Burma Trough for a better prediction of the interannual variation of northern Indochina's biomass burning activity and its downwind impact on PM_{10} at LABS in Taiwan. However, for the shorter time scale variations, the role of the India-Burma Trough in the modulation of biomass burning in Indochina and its downwind impacts might be different than that revealed in this study. Further examinations are suggested in the future to explore this issue in detail.

Acknowledgments

The NCEP-DOE Reanalysis 2 data set was provided by the NOAA/OAR/ESRL PSD, Boulder, CO, USA, from their website at http://www.esrl.noaa.gov/psd/. The MODIS fire count data and the GFED4s biomass burning emissions were provided by http://reverb.echo.nasa.gov and http://globalfiredata.org/data.html, respectively. The authors thank Ritesh Gautam and anonymous reviewers for their comments and suggestions which greatly improved the manuscript. This research was supported by the Ministry of Science and Technology of Taiwan under MOST 104-2111-M-003-001, MOST 105-2119-M-003-002, and MOST 105-2625-M-003-002. S.-H. Wang was supported by MOST 104-2111-M-008-009. N.-H. Lin was supported by MOST 103-2111-M-008-001 and EPA-105-U1L1-02-A046 funded by Taiwan Environmental Protection Administration.

References

Chen, T. C., M. C. Yen, and M. Murakami (1988), The water vapor transport associated with the 30–50 day oscillation over the Asian monsoon regions during 1979 summer, *Moon Weather Rev.*, *116*, 1983–2002.

Cheng, F. Y., Z. M. Yang, C. F. O. Yang, and F. Ngan (2013), A numerical study of the dependence of long-range transport of CO to a mountain station in Taiwan on synoptic weather patterns during the Southeast Asia biomass burning season, *Atmos. Environ.*, *78*, 277–290.

Chuang, M. T., et al. (2015), Simulating the transport and chemical evolution of biomass burning pollutants originating from Southeast Asia during 7-SEAS/2010 Dongsha experiment, *Atmos. Environ.*, *112*, 294–305.

Dong, X., and J. S. Fu (2015), Understanding interannual variations of biomass burning from Peninsular Southeast Asia, part II: Variability and different influences in lower and higher atmosphere levels, *Atmos. Environ.*, *115*, 9–18.

Duncan, B. N., R. V. Martin, A. C. Staudt, R. Yevich, and J. A. Logan (2003), Interannual and seasonal variability of biomass burning emissions constrained by satellite observations, *J. Geophys. Res.*, *108*(D2), 4040, doi:10.1029/2002JD002378.

Food and Agriculture Organization of the United Nations (FAO) (2016), FAOSTAT data base. [Available at http://faostat.fao.org].

Gautam, R., N. C. Hsu, T. F. Eck, B. N. Holben, S. Janjai, T. Jantarach, S. C. Tsay, and W. K. Lau (2013), Characterization of aerosols over the Indochina peninsula from satellite-surface observations during biomass burning pre-monsoon season, *Atmos. Environ.*, *78*, 51–59.

Giglio, L. (2013), MODIS collection 5 active fire product user's guide version 2.5. 61 pp. [Available at http://modis-fire.umd.edu/files/MODIS_Fire_Users_Guide_2.5.pdf.]

Giglio, L., J. Descloitres, C. O. Justice, and Y. J. Kaufman (2003), An enhanced contextual fire detection algorithm for MODIS, *Remote Sens. Environ.*, *87*, 273–282.

Giglio, L., J. T. Randerson, G. R. van der Werf, P. S. Kasibhatla, G. J. Collatz, D. C. Morton, and R. S. DeFries (2010), Assessing variability and long-term trends in burned area by merging multiple satellite fire products, *Biogeosciences*, *7*, 1171–1186.

Giglio, L., J. T. Randerson, and G. R. van der Werf (2013), Analysis of daily, monthly, and annual burned area using the fourth-generation global fire emissions database (GFED4), *J. Geophys. Res. Biogeosci.*, *118*, 317–328, doi:10.1002/jgrg.20042.

Hannachi, A., I. Jolliffe, and D. Stephenson (2007), Empirical orthogonal functions and related techniques in atmospheric science: A review, *Int. J. Climatol.*, *27*, 1119–1152.

Hong, Y., K. L. Hsu, S. Sorooshian, and X. Gao (2005), Improved representation of diurnal variability of rainfall retrieved from the Tropical Rainfall Measurement Mission Microwave Imager adjusted Precipitation estimation from Remotely Sensed Information Using Artificial Neural Networks (PERSIANN) system, *J. Geophys. Res.*, *110*, D06102, doi:10.1029/2004JD005301.

Huang, K., J. S. Fu, N. C. Hsu, Y. Gao, X. Dong, S. C. Tsay, and Y. F. Lam (2013), Impact assessment of biomass burning on air quality in Southeast and East Asia during BASE-ASIA, *Atmos. Environ.*, *78*, 291–302.

Huang, W. R., and J. C. L. Chan (2012), Seasonal variation of diurnal and semidiurnal variation of rainfall over southeast China, *Clim. Dyn.*, *39*, 1913–1927.

Huang, W. R., and S. Y. Wang (2014), Impact of land-sea breezes at different scales on the diurnal rainfall in Taiwan, *Clim. Dyn.*, *43*, 1951–1963.

Huffman, G. J., R. F. Adler, D. T. Bolvin, G. Gu, E. J. Nelkin, K. P. Bowman, Y. Hong, E. F. Stocker, and D. B. Wolff (2007), The TRMM multisatellite precipitation analysis (TMPA): Quasi-global, multiyear, combined-sensor precipitation estimates at fine scales, *J. Hydrometeorol.*, *8*(1), 38–55.

Kanamitsu, M., W. Ebisuzaki, J. Woollen, S. K. Yang, J. J. Hnilo, M. Fiorino, and G. L. Potter (2002), NCEP–DOE. AMIP-II Reanalysis (R-2), *Bull. Am. Meteorol. Soc.*, *83*, 1631–1643.

Kim Oanh, N. T., and K. Leelasakultum (2011), Analysis of meteorology and emission in haze episode prevalence over mountain-bounded region for early warming, *Sci. Total Environ.*, *409*, 2261–2271.

Lee, C. T., et al. (2011), The enhancement of $PM_{2.5}$ mass and water-soluble ions of biosmoke transported from Southeast Asia over the Mountain Lulin site in Taiwan, *Atmos. Environ.*, *45*(32), 5784–5794.

Li, X. Z., and W. Zhou (2016), Modulation of the interannual variation of the India-Burma Trough on the winter moisture supply over southwest China, *Clim. Dyn.*, *46*, 147–158.

Lin, N. H., et al. (2013), An overview of regional experiments on biomass burning aerosols and related pollutants in Southeast Asia: From BASE-ASIA and Dongsha experiment to 7-SEAS, *Atmos. Environ.*, *78*, 1–19.

Ou Yang, C. F., N. H. Lin, C. C. Lin, S. H. Wang, G. R. Sheu, C. T. Lee, R. C. Schnell, P. M. Lang, T. Kawasato, and J. L. Wang (2014), Characteristics of atmospheric carbon monoxide at a high-mountain background station in East Asia, *Atmos. Environ.*, *89*, 613–622, doi:10.1016/j.atmosenv.2014.02.060.

Promchote, P., S. Y. S. Wang, and P. G. Johnson (2015), The 2011 great flood in Thailand: Climate diagnostics and Implications from climate change, *J. Clim.*, *29*, 367–379, doi:10.1175/JCLI-D-15-0310.1.

Reid, J. S., et al. (2013), Observing and understanding the Southeast Asian aerosol system by remote sensing: An initial review and analysis for the Seven Southeast Asian Studies (7SEAS) program, *Atmos. Environ.*, *122*, 403–468.

Sanap, S. D., and G. Pandithurai (2015), The effect of absorbing aerosols on Indian monsoon circulation and rainfall: A review, *Atmos. Res.*, *164-165*, 318–327.

Shi, Y., and Y. Yamaguchi (2014), A high-resolution and multi-year emissions inventory for biomass burning in Southeast Asia during 2001-2010, *Atmos. Environ.*, *98*, 8–16.

Sonkaew, T., and R. Macatangay (2015), Determining relationships and mechanisms between tropospheric ozone column concentrations and tropical biomass burning in Thailand and its surrounding regions, *Environ. Res. Lett.*, *10*, 065009, doi:10.1088/1748-9326/10/6/.

Suo, M. Q., and Y. H. Ding (2009), The structure and evolution of the wintertime southern branch trough in the subtropical westerlies [in Chinese], *Chin. J. Atmos. Sci.*, *33*(3), 425–442.

Suo, M. Q., Y. H. Ding, and J. Y. Wang (2008), Relationship between Rossby wave propagation in southern branch of westerlies and the formation of the southern branch trough in wintertime [in Chinese], *J. Appl. Meteorol. Sci. 19*(6), 731–740.

Wang, B., and Q. Zhang (2002), Pacific-East Asian teleconnection. Part II: How the Philippine Sea anomalous anticyclone is established during El Niño development, *J. Clim.*, *15*, 3252–3265.

Wang, S. H., et al. (2015), Vertical distribution and columnar optical properties of springtime biomass burning aerosols over northern Indochina during 2014 7-SEAS campaign, *Aerosol Air Qual. Res.*, *15*, 2037–2050, doi:10.4209/aaqr.2015.05.0310.

Wang, T. M., S. Yang, Z. P. Wen, R. G. Wu, and P. Zhao (2011), Variations of the winter India-Burma Trough and their links to climate anomalies over southern and eastern Asia, *J. Geophys. Res.*, *116*, D23118, doi:10.1029/2011JD016373.

Yen, M. C., C. M. Peng, T. C. Chen, C. S. Chen, N. H. Lin, R. Y. Tzeng, Y. A. Lee, and C. C. Lin (2013), Climate and weather characteristics in association with the active fires in northern Southeast Asia and spring air pollution in Taiwan during 2010 7-SEAS/Dongsha Experiment, *Atmos. Environ.*, *78*, 35–50.

Yu, J.-Y., N.-H. Lin, H.-H. Hsieh, and T.-S. Lin (2008), A cluster analysis of the springtime forward trajectories arising from Southeast Asia and the climate influence [in Chinese with English abstract], *Atmos. Sci.*, *36*, 287–301.

Zhou, T., R. Yu, H. Chen, A. Dai, and Y. Pan (2008), Summer precipitation frequency, intensity, and diurnal cycle over China: A comparison of satellite data with rain gauge observations, *J. Clim.*, *21*, 3997–4010.

Zhou, W., J. C. L. Chan, W. Chen, J. Ling, J. G. Pinto, and Y. P. Shao (2009), Synoptic-scale controls of persistent low temperature and icy weather over southern China in January 2008, *Moon Weather Rev.*, *137*, 3978–3991.

Zong, H. F., C. L. Bueh, J. Wei, and L. T. Chen (2012), Intensity of the trough over the Bay of Bengal and its impact on the southern China precipitation in winter, *Atmos. Ocean Sci. Lett.*, *5*(3), 246–251.